ChemComm

Accepted Manuscript

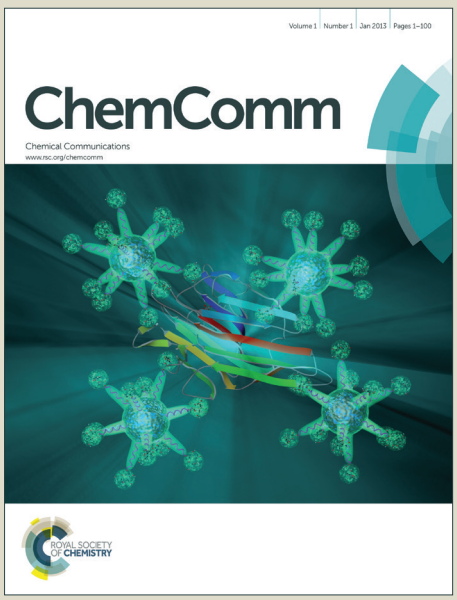

ROYAL SOCIETY OF CHEMISTRY

www.rsc.org/chemcomm

Journal Name

COMMUNICATION

Raman/Fluorescence Dual-Sensing and Imaging of Intracellular pH Distribution

Received 00th January 20xx,
Accepted 00th January 20xx

DOI: 10.1039/x0xx00000x

www.rsc.org/

Yue Cao, Ruo-Can Qian, Da-Wei Li, Yi-Tao Long*

Herein, a pH-sensitive probe has been designed based on DNA modified gold nanoparticles (AuNPs) for Raman/fluorescence dual-imaging of the intracellular pH distribution. In acidic environment of cancer cell, the configuration change of DNA on probe surface could turn "on" Raman/fluorescence signals simultaneously.

Cancer cell is characterized by uncontrolled cell growth, invasion of surrounding tissues and abnormal acidic intracellular pH values.[1] Therefore, it is an urgent need to develop sensors for the detection of intracellular pH.[2] Owning to the significance of intracelluar pH distribution, various fluorescent indicators[3, 4] and functionalized nanoparticles[5, 6] have been developed for measuring intracellular pH. Among them, gold nanoparticles (AuNPs) are especially attractive due to its unique properties, easy functionalization, good stability and biocompatibility.[7-9] AuNPs can be applied as excellent substrates for surface-enhanced Raman scattering (SERS) detection to carry Raman signalling molecules.[10] In addition, AuNPs are also employed as carriers for fluorescent dye for the intracellular fluorescent imaging[11]. For most of the reported AuNP probes, they only possess one kind of signals, like fluorescence or Raman, each with certain advantages and limitations.[12] Fluorescent probes have the advantage of high specificity. However, the fluorescence imaging of living cells suffers from the photobleaching, non-ignorable background signal and unstable. For in view of the advantages of Raman, they can avoid photobleaching due to the extremely short lifetimes of Raman scattering, and that can provide the abundant vibrational information of molecules, but the targeting ability is not so well as fluorescent probes.[13] Thus, it is essential to develop novel nanoprobes combining the virtues of fluorescence and Raman.[14] Up to now, there is no report about the use of Raman/fluorescence dual-imaging for the monitoring of intracellular pH distribution. Therefore, we proposed a Raman/fluorescence dual-sensing strategy in order to establish a better platform for the detection of pH distribution in single living cells.

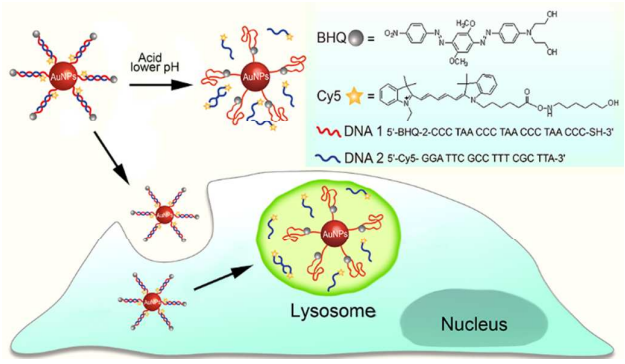

Figure 1. Schematic representation of the in situ Raman/fluorescence dual-imaging of intracellular pH-distribution based on the AuNP probe.

Here we designed a novel pH-sensitive probe using AuNPs as the substrates. A double-strand DNA structure was functionalized on the surface of AuNPs, which was hybridized by DNA-1 and its complementary strand DNA-2. The DNA-1 is a cytosine (C)-rich single strand with a thiol-labelled 3'-end for the connection to the AuNPs, and its 5'-end was tagged by a Raman signaling molecule, 2,2'-((4-((E)-(2,5-dimethoxy-4-((E)-(4-nitrophenyl)diazenyl)phenyl)diazenyl)phenyl)azanediyl)diethanol (BHQ-2). While DNA-2 was marked with fluorophore Cy5 at the 5'-end, whose fluorescence was quenched by both AuNP and BHQ-2 due to the fluorescence resonance energy transfer (FRET).[15] In acidic pH, the DNA-1 strand could be transformed from a straight strand to a tetrameric-structured i-motif structure. With the conformational change, the BHQ-2 molecules were dragged closer to the surface of AuNPs, which enhanced the Raman response; at the same time, the Cy5-tagged DNA-2 was released away from the AuNPs, which turned "on" the fluorescence signal. Taking human cervical cells (HeLa) as a model, after endocytosis of the AuNP probe,

Key Laboratory for Advanced Materials & Department of Chemistry, East China University of Science and Technology, 130 Meilong Road, Shanghai, 200237, P. R. China.
E-mail: ytlong@ecust.edu.cn
†Electronic Supplementary Information (ESI) available: Detailed description of the material, density functional theory calculations and supplementary experimental. See DOI: 10.1039/x0xx00000x

strong Raman and fluorescent signals could be observed due to the acid intracellular environment, which realized the in situ Raman/fluorescence dual- imaging of the pH distribution in single cells (Figure 1). The practicality of the probe was demonstrated by the application of distinguishing cancer cell from normal cells, thus provided a powerful highly efficient photosensitizers for cancer diagnosis.

AuNPs were synthesized by a reported aqueous phase method.[16] The transmission electron microscopic (TEM) image of AuNPs showed an average diameter of 60 nm with narrow distribution (Figure 2a). After functionalized the probe with the double stand hybridized by DNA-1 and DNA-2, the UV-vis spectrum of probe solution showed the characteristic peak of DNA at 260 nm and AuNPs at 550 nm (Figure 2b), which demonstrated the successful functionalization of DNA on the surface of AuNPs. In order to monitor the response of the probe in acidic pH, Raman spectra and fluorescence spectra were recorded at physical pH or acidic pH at different time points, respectively (Figure S1a and Figure S2). With the increasing incubation time, both Raman/fluorescence signals were strongly increased under acidic pH simultaneously. At the beginning, no fluorescence was detected at the excitation wavelength of 600 nm for Cy5, suggesting the quenched status of Cy5 by AuNPs. The fluorescence intensity increased over time and tended to a constant value after 25 min (Figure S1 b). Since the fluorescence and Raman signals no longer changed after 20 min, we choose 25 min as the optimized reaction time. Under the optimized reaction time, the Raman/fluorescence spectra were recorded (Figure 2c and Figure 2d). The Raman/fluorescence signals were turned "on" at pH 5.0, which demonstrated structure transformation of the DNA-1 to i-motif tetrameric structure, causing the release of Cy5-tagged DNA-2. In addition, both of the fluorescence spectra (Figure S3) and the Raman spectra (Figure S4) of the probe were detected under a series of different pH values, which displayed strong fluorescence signals and obvious Raman peaks under pH 5.0, with weak signals detected above pH 5.0. Thus pH 5.0 could be regarded as a threshold of the structure switch of DNA-1 to i-motif.

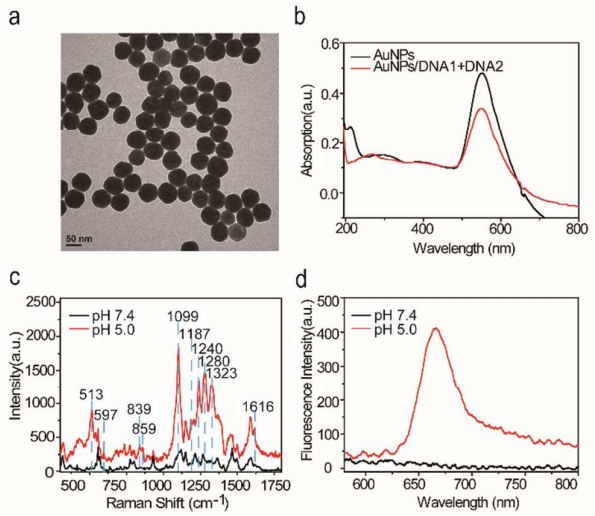

Figure 2. (a) TEM image of AuNPs. (b) UV-vis spectra of AuNPs (2 nM) and probe (2 nM). (c, d) Raman (c) and Fluorescence (d) spectra of probe in 0.01 M PBS buffer pH 7.4 and pH 5.0 PBS after 25 min.

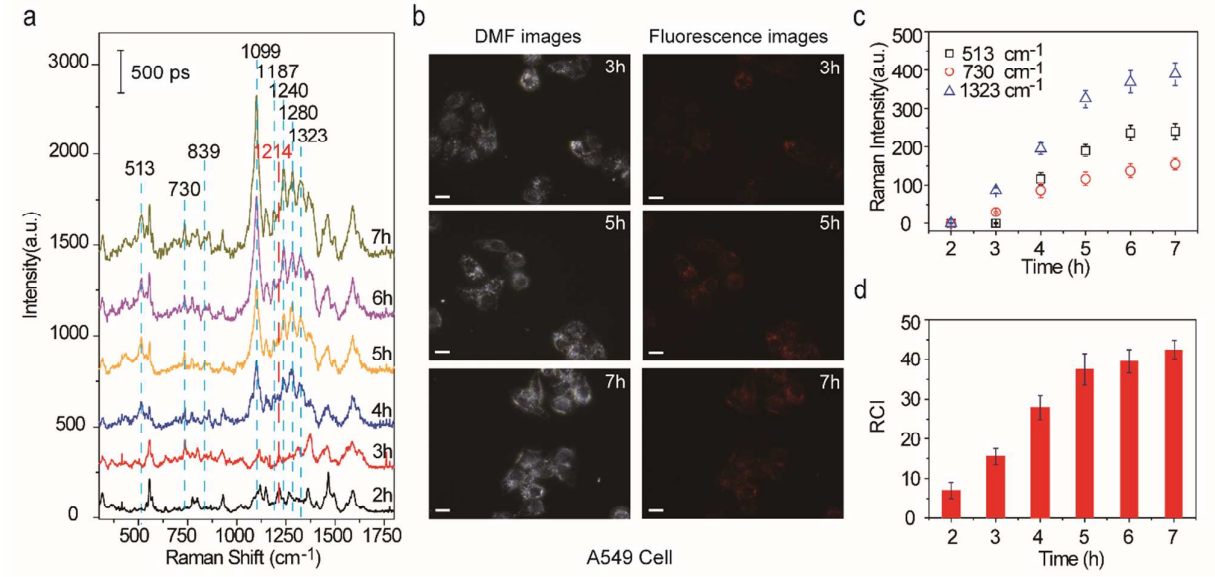

Figure 3. (a) Real-time monitoring of the SERS signals of BHQ-2 in A549 cells treated with 50 μL probe solution after different times. (b) Fluorescence images of A549 cells treated with 50 μL probe solution after different times (scale bar: 10 μm). (c) Plots of Raman intensities at 593 cm^{-1}; 730 cm^{-1} and 1323 cm^{-1} versus after different times. (d) Increase of the relative average red channel intensity (RCI) intensity of Cy5 fluorescence in images over time.

For cell imaging, A549 cells (lung adenocarcinoma epithelial cell) were cultured in a confocal dish for 24 h, and 50 μL probe solution was then added to the dish to obtain the Raman signals (Figure 3a) and fluorescence images (Figure 3b) respectively at different time points. Initially, Raman signals were very low within 3 h. After 4 h, several characteristic peaks appeared, and the peak intensity kept increasing due to the structure switch of DNA-1 to i-motif, which indicated the acidic

intracellular pH of A549 cells. It could be further demonstrated by corresponding fluorescence images of probe treated A549 cells. As shown in Figure 3b, after 3 h of incubation, the probe appeared in the cytoplasm, which could be observed under dark-field microscope (DFM), and the fluorescence signal of Cy5 was quite weak under the observation of fluorescence microscope. The fluorescence intensity increased with the increasing incubation time, which illustrated the release of Cy5-tagged DNA-2 from the surface of AuNPs, confirming the acidic pH in A549 cells. Plots of Raman shift intensities vs. incubation time at 513 cm^{-1}; 730 cm^{-1} and 1323 cm^{-1} was shown in Figure 3c. The average red channel intensity (RCI) within the cell area was shown in Figure 2d read by Adobe Photoshop software from the Cy5 fluorescence images. (Figure 3b). For the parsing of Raman spectra, we focused on the peaks from 300 to 1800 cm^{-1}. Furthermore, we supplemented DFT calculations to assign the SERS peaks of the BHQ-2 in the Table S1. After the A549 cells were treated with the probe, the band at 1214 cm^{-1} corresponding to O-C=O stretch was decreased significantly, and disappeared after 4 h. Since only Cy5 contains O-C=O structure, this phenomenon indicated the release of Cy5-tagged DNA-2 from the AuNPs. In addition, new vibrational Raman bands at 513, 839, 1099 cm^{-1} appeared at after 4 h, corresponding to the NO2, N=N, C-N, respectively. As well as several other characteristic bands at 730, 1240, 1280 and 1323 cm^{-1} corresponding to the CC, C=N=N, N=N, C=N, respectively, probably due to the closer distance between the BHQ-2 molecules and the surface of AuNPs. Therefore, the Raman spectra demonstrated the structure transformation of DNA-1 in acidic pH.

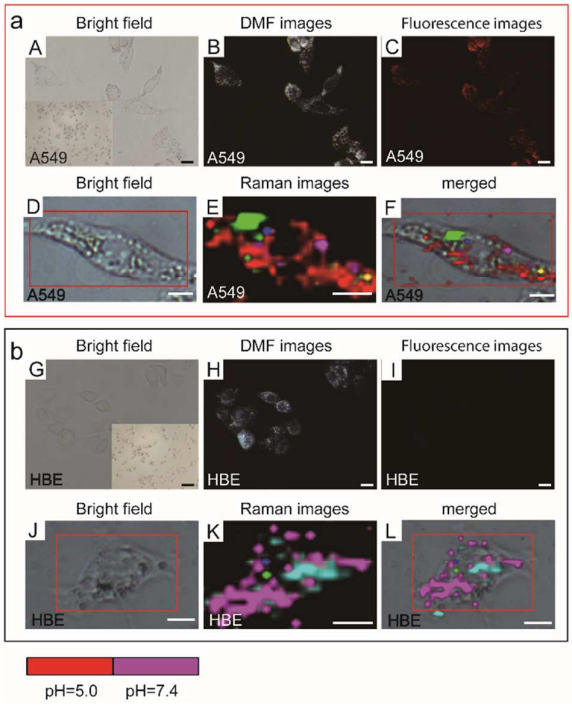

Figure 4. Microscopic images of (a) A549 and (b) HBE cells incubated with 50 μL probe solution for 7 h. (A,D,G&J: bright-field images; B&H: DFM images; C&I: fluorescence images; E&K: Raman images; F&L: bright-field merged Raman images; scale bar: 10 μm).

The feasibility of the probe for in situ dual imaging of the pH distribution in single cells was further explored in A549 and a normal cell line HBE (normal human bronchial epithelial cells). As shown in Figure 4, after 7 h incubation with the probe, a large amount of probe particles appeared in A549 cells (Figure 4a B),and the fluorescence signal of Cy5 was quite strong (Figure 4a C). The Raman image of a single A549 cell showed an acidic intracellular environment with red areas distributed with cytoplasm (Figure 4E), showing a strong Raman response (Figure S5a). As a contrast, HBE did not show any fluorescence signals under probe treatment (Figure 4I). In Raman image of HBE, most of the intracellular areas were purple colored (Figure 4K), showed little Raman response (Figure S5b), which indicated neutral pH in HBE cells. The distinct Raman/fluorescence responses of tumor and normal cells under the probe treatment demonstrated the successful application of the proposed strategy in distinguishing cancer cell from normal cells. Thus, this strategy has the potential for cancer diagnostic and therapy. The cytotoxicity of the probe was detected by MTT analysis. The cells exhibited high viability even after 8 h incubation (Figure S6), demonstrating the low cytotoxicity of the designed probe.

In conclusion, we presented a pH-sensitive AuNP probe for Raman/fluorescence dual-imaging of intracellular pH distribution. This strategy integrated the advantages of Fluorescence and Raman analysis, realizing the in situ observation of intracellular pH-distribution at single cell level. The practicality of the proposed strategy is confirmed by the successful application of distinguishing cancer cell from normal cells with different intracellular pH levels. Compared with reported methods, the proposed probe realized a one-step incubation process, providing a pH-sensitive Raman/ fluorescence dual-imaging strategy with a low background. This work promotes the understanding of physical properties of cancer cell, provides a new way for the design and preparation of intracellular imaging nanomaterials, and inspires the development of new tools for cancer diagnosis and therapy.

This research was supported by the National Basic Research 973 Program (2013CB733700), NSFC (21421004, 21125522, 21327807, 21575041), the Shanghai Pujiang Program Grant of China (12JC1403500), the Shanghai Municipal Natural Science Foundation (14ZR1410800), the Fundamental Research Funds for the Central Universities (WB1113005) and the China Postdoctoral Science Foundation (2015M570335).

Notes and references

1 L. Chen, X. L. Qu, M. Cao, Y. Y. Zhou, W. Li, B. H. Liang, W. G. Li, W. M. He, C. C. Feng, X. Jia and Y. H. He, *Sci. Rep.*, 2013, **3**, 3368.
2 A. Awan, E. Wang, Z. Yu, S. Moksong, H. Bari, Q. Cui, E. O. Purisima, S. Yang, F. Yan and S. Chowdhury, *IET. Syst. Biol.*, 2007, **1**, 292-297.
3 J. T. Zhang, M. Yang, C. Li, N. Dorh, F. Xie, F. T. Luo, A. Tiwari and H. Y. Liu, *J. Mater. Chem. B*, 2015, **3**, 2173-2184.
4 J. W. Tian, L. Ding, H. J. Xu, Z. Shen, H. X. Ju, L. Jia, L. Bao and J. S. Yu, *J. Am. Chem. Soc.*, 2013, **135**, 18850-18858.

5 F. Wang, R. G. Widejko, Z. Yang, K. T. Nguyen, H. Chen, L. P. Fernando, K. A. Christensen and J. N. Anker, *Anal. Chem.*, 2012, **84**, 8013-8019.
6 L. Sun, Z. Zhang, S. Wang, J. Zhang, H. Li, L. Ren, J. Weng and Q. Zhang, *Nanoscale Res Lett.*, 2008, **4**, 216-220.
7 Nathaniel L. Rosi and C. A. Mirkin, *Chem. Rev.*, 2005, **105**, 1547-1562.
8 Y. C. Cao, R. Jin and C. A. Mirkin, *Science*, 2002, 297, 1536-1540.
9 C. S. T. Jwa-Min Nam, Chad A. Mirkin, *Science*, 2003, **301**, 1884-1886.
10 X. P. Wei, S. Su, Y. Y. Guo, X. X. Jiang, Y. L. Zhong, Y. Y. Su, C. H. Fan, S. T. Lee and Y. He, *Small*, 2013, **9**, 2493-2499, 2652.
11 R. C. Qian, L. Ding, L. W. Yan, M. F. Lin and H. X. Ju, *Anal. Chem.*, 2014, **86**, 8642-8648.
12 Y. Wang, B. Yan and L. Chen, Chemical reviews, 2013, **113**, 1391-1428.
13 Y. L. Chen, L. Ding, J. Q. Xu, W. Y. Song, M. Yang, J. J. Hua, and H. X. Ju, Chem. Sci., 2015, **6**, 3769-3774.
14 B. Kang, L. A. Austin and M. A. El-Sayed, Nano Lett., 2012, **12**, 5369-5375.
15 R. C. Qian, L. Ding, L. W. Yan, M. F. Lin and H. X. Ju, J. Am. Chem. Soc., 2014, **136**, 8205-8208.
16 K. C. Grabar, R. G. Freeman, M. B. Hommer and M. J. Natan, Anal. Chem., 1995, **67**, 735-743.

The table of contents:

Raman/Fluorescence Dual-Sensing and Imaging of Intracellular pH Distribution

Yue Cao, Ruo-Can Qian, Da-Wei Li, Yi-Tao Long*

A pH-sensitive probe has been designed based on DNA modified gold nanoparticles (AuNPs) for Raman/fluorescence dual-imaging of the intracellular pH distribution.